SIMULATIONS OF CRACK MEANDERING AND CRACK BRANCHING IN INTERGRANULAR CREEP FRACTURE

Y. Kaim, P.R. Onck, E. van der Giessen
University of Groningen, Department of Applied Physics, Micromechanics group
Nijenborgh 4, 9747 AG Groningen, The Netherlands
Y.Kaim@phys.rug.nl, P.R.Onck@phys.rug.nl, Giessen@phys.rug.nl

Abstract

We present a numerical model for intergranular creep fracture of a single notched specimen under tensile loading. The model accounts for the nucleation and growth of grain boundary cavities, their coalescence to microcracks and the formation of macroscopic cracks until the specimen breaks. Typical results are presented for ductile and for brittle crack growth, and their sensitivity to grain-to-grain fluctuations in properties is briefly presented. The effect of boundary conditions on fracture path is emphasized.

Introduction

Crack growth in heterogeneous materials is often a very complex process, featuring many different physical mechanisms. The fracture mechanisms in different material classes have their own time-scale and stress dependence, leading to a stochastic and material-specific appearance of the fracture surface. Crack surfaces often have a complex meandering structure with a large number of small crack branches that accompany growth of the main crack. These surfaces appear to be fractal [1] in many cases [2]. Surprisingly, the parameter that describes the degree of fractality is very similar for a wide range of material systems, having distinctly different fracture mechanisms [1,2]. The current work aims at elucidating this by studying the conditions that determine the appearance of the fracture surface in creeping polycrystalline materials.

Creep fracture in polycrystalline materials starts by the nucleation and growth of grain boundary cavities, which ultimately coalesce to form a grain boundary microcrack. Crack advance occurs when these microcracks link up. The damage process entails various competing mechanisms, including the competition between diffusion and creep, grain boundary sliding and the (poorly understood) stress-state dependence of cavity nucleation. Recently, a numerical multi-grain model has been developed that takes into account these mechanisms, enabling the simulation of macroscopic creep crack growth in a polycrystalline aggregate, assuming small-scale damage conditions [3,4]. In these studies, however, no crack meandering was observed. In the current analysis, we use the same constitutive equations describing creep deformation and damage development as in [3,4], but relax the small-scale damage assumption by explicitly modelling the geometry of the specimen. We consider a single-edge notched specimen and investigate the effect of a number of material and loading parameters on the occurrence of crack branching and meandering.

Model description

We consider a single-edge notched specimen loaded by a uniform tensile stress σ_∞ (see Fig. 1a). The specimen dimensions are specified by its height $H = 50d$, width $W = 66d$ and crack length $a = 33d$ (giving $a/W = 0.5$), where $d = 3R$ is the grain size (see Fig. 1b). The specimen is discretized by continuum elements in the far-field region, which is connected to a

process-window near the crack-tip in which the polycrystalline microstructure is represented by grain elements, connected by grain boundary elements (see Fig. 1b). The hexagonal grain elements account for elasticity and creep inside the grains and the grain boundary elements account for cavitation and grain boundary sliding. For a detailed discussion on the numerical implementation and constitutive equations governing the deformation and damage mechanisms, the reader is referred to [3]. Here only a summary is given.

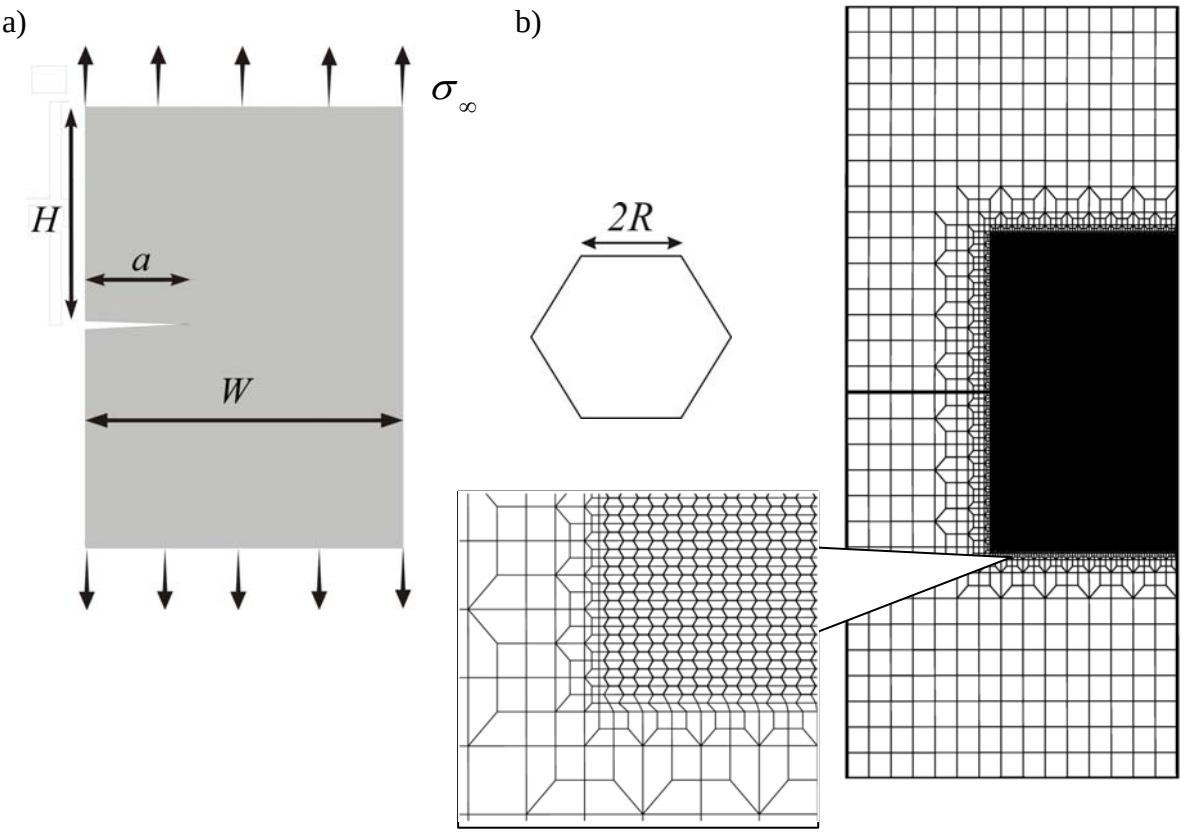

FIGURE 1. a) Specimen geometry, b) Finite element mesh, with separate grains modeled inside the process zone.

Creep deformation of the grains is governed by the Norton creep law

$$\dot{\varepsilon}_e = B\sigma_e{}^n, \tag{1}$$

where $\dot{\varepsilon}_e$ and σ_e are the effective strain rate and stress, $B = \dot{\varepsilon}_0 / \sigma_0{}^n$ is the creep parameter, n the creep exponent, and $\dot{\varepsilon}_0$ and σ_0 reference strain rate and stress quantities. Cavity nucleation is described by

$$\dot{N} = F_n \left(\frac{\sigma_n}{\Sigma_0} \right)^2 \dot{\varepsilon}_0, \tag{2}$$

where N is the cavity density, F_n a material parameter, Σ_0 a normalization factor and σ_n the normal facet stress. Cavity growth is governed by diffusion and creep deformation, whose relative contribution can be described by the length scale

$$L = \left[D\Sigma / \dot{E} \right]^{1/3}, \tag{3}$$

where D is the diffusion coefficient, $\Sigma = \sigma_\infty (1 - a/W)^{-1}$ the net-section stress and $\dot{E} = B\Sigma^n$ the net-section creep rate, in accordance with eq. (1).

Results and discussion

The material parameters are chosen as follows. The applied stress is specified as $\sigma_\infty / E = 1.6 \times 10^{-4}$ where E is Young's modulus. The time is normalized by the creep reference time $t_R = 1/\dot{E}$. The reference stress Σ_0 in (2) is chosen to be equal to Σ and the creep exponent $n = 5$. We consider a brittle case, where the diffusion coefficient specified by $L/d = 0.042$ is relatively large, and a more ductile case for which $L/d = 0.19$. The nucleation parameter F_n in (2) is chosen such that the size of the damage zone (number of nucleated facets) at the moment the first microcrack appears is the same for the ductile and brittle case, resulting in $F_n d^2 = 0.24 \times 10^4$ and $F_n d^2 = 0.21 \times 10^3$ for the ductile and brittle case, respectively. To introduce randomness in the simulations, F_n and B are chosen at random from a Gaussian distribution; for details see [3,4]. Most cases have stress-controlled boundary conditions, while one case is displacement controlled, where the vertical displacement rate is specified through $v_b = \left(\sqrt{3}/2\right)^n 2HB\sigma_\infty{}^n$, so that the creep rates under both boundary conditions are identical in the absence of a crack.

The initiation of the crack in the brittle case (Fig. 2a) is accompanied by a large damage zone that gradually decreases in later stages of the fracture process (Fig. 2b). This is caused by bending during the later stages of crack growth which is allowed by the stress controlled boundary conditions (see Figs. 2c-d). One dominant crack forms having a surface that contains a large number of branches with a characteristic size much smaller than the crack length. In the ductile case, with the same initial conditions, branching starts right from the beginning (Fig. 3a), and fracture is accompanied by a competition of different branches that highly depends on the randomness in the material properties (see Figs. 3b-d).

To emphasize this branching behaviour Figs. 4a and 4c show the topology of the "main crack" plotted on the reference configuration for the ductile and brittle case respectively. These topology plots have been created by marking the fractured grain boundaries that belong to the "main crack" defined as the percolation of neighboring microcracks connected to each other, starting form the initial crack tip. Figure 4b shows the crack mouth opening at the left side of the specimen versus crack length, being the projection of the crack topology on the horizontal axis. The points a, b, c on Fig. 4b correspond to the crack state shown in Figs. 2a-c for the brittle case and in Figs. 3a-c for the ductile case. The beginning of the brittle fracture (Fig. 4b) is characterized by fast growth of the crack with relatively small crack opening displacement, while during ductile fracture branching occurs, which leads to a relatively large opening displacement for a given crack length even at the beginning of the fracture process. Further crack growth develops with approximately the same rate for the brittle and ductile case. This is probably a result of the fact that after a certain amount of crack advance and opening further crack growth is controlled by the specimen rotation.

The effect of randomness was introduced in the current model by using a Gaussian distribution for the creep parameter B in (1) and the nucleation factor F_n in (2). To investigate the effect of the specific random distribution on the overall crack growth behaviour, we performed two additional calculations with a different random realization. The topologies are shown in Figs. 5a and 5b for the brittle case and in Figs. 5c and 5d for the

ductile case, still showing one dominant crack and branched crack growth, respectively. The influence of the "randomness" on the overall crack growth behaviour for the ductile fracture is somewhat bigger than in the brittle case, but for both cases the scatter in crack opening and length remains small (see Fig. 5e).

The previous discussion was related to a fracture process with stress-controlled boundary conditions. To study the effect of the rotational degrees of freedom, we also performed a calculation with displacement controlled boundary conditions for the ductile set of material parameters. As can be observed (Fig. 6) the fracture process in this case has a totally different character. The damage zone in Fig. 6a is much larger compared to Fig. 3a, forming a V-shaped region instead of a more-or-less circular region. The crack opening is much smaller for a certain amount of crack growth which can be directly related to the displacement controlled boundary conditions that also not allow for rotation of the specimen. Note, however, that stronger conclusions can not be drawn at this stage, since the net-section stress for the displacement controlled conditions is only half that of the stress controlled case.

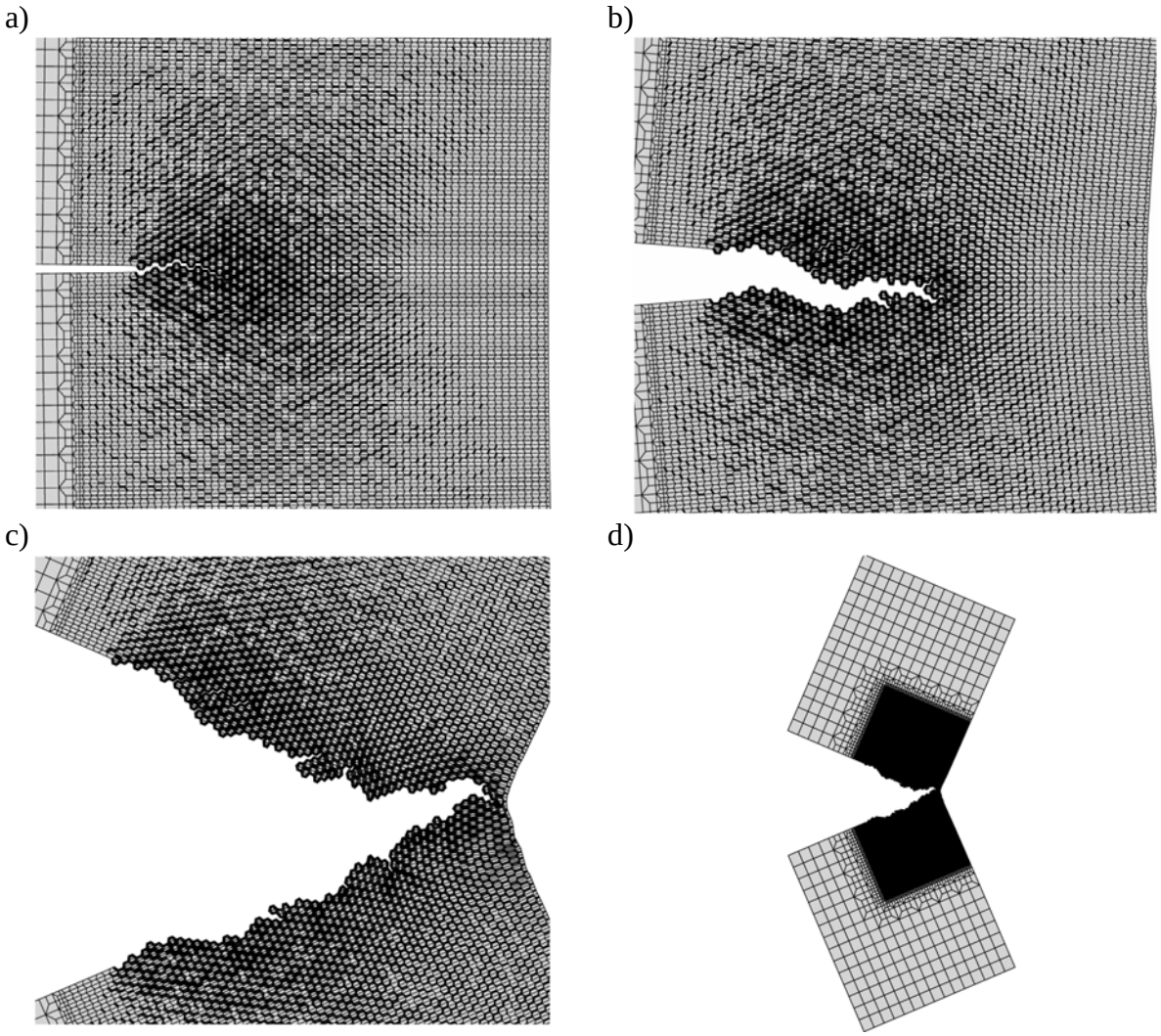

FIGURE 2. Snapshots during brittle crack growth with $L/d = 0.19$, $F_n d^2 = 0.24 \times 10^4$: a) $t/t_{ref} = 5.54 \times 10^{-2}$; b) $t/t_{ref} = 5.81 \times 10^{-2}$; c) $t/t_{ref} = 6.74 \times 10^{-2}$; d) $t/t_{ref} = 6.74 \times 10^{-2}$. The thickness of plotted grain boundaries scales with the amount of cavitation damage.

Concluding remarks

Modeling a full specimen is a significant advancement over small-scale damage studies [4] in that they allow for crack growth until the specimen breaks into two pieces. Also, it breaks the symmetry in the small-scale damage problem which stabilizes geometrically-induced crack growth. Yet, the results presented here show that the damage pattern and final fracture path depend quite sensitively on the type of boundary conditions. Although the model is deterministic – based on physically motivated models of the fracture mechanisms, the final crack path is complex, involving crack branching and meandering. The preliminary studies reported here suggest that the details of the crack path are controlled by statistical fluctuations of the material properties, while overall characteristics such as crack length and opening distance are fairly insensitive. Although these features need to be studied to greater depth, it seems fair to conclude that this kind of modeling promises to pave the way to exploring statistical properties of fracture surfaces and to relate them to experimental findings of fractality.

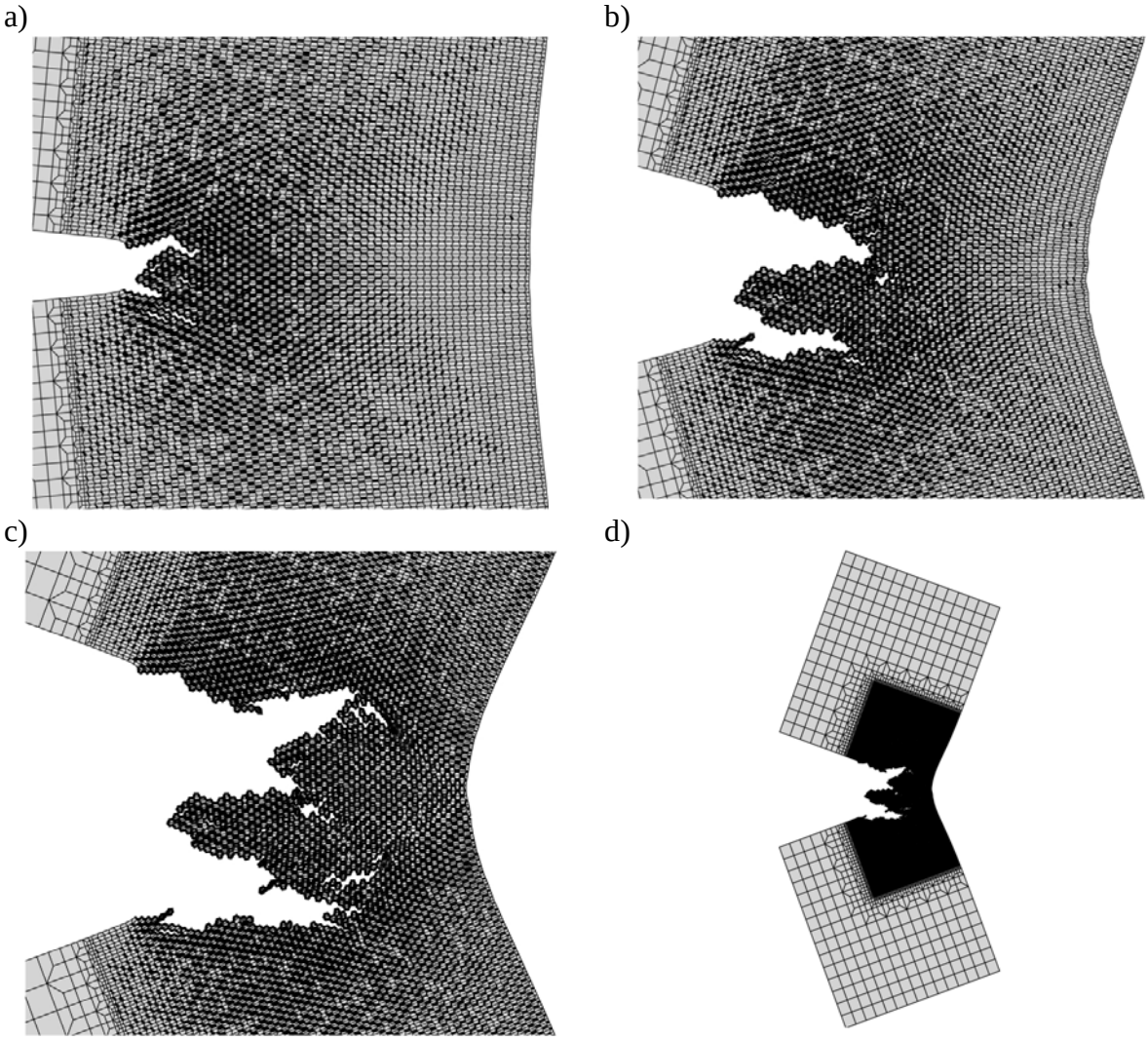

FIGURE 3. Snapshots during ductile crack growth with $L/d = 0.042$, $F_n d^2 = 0.21\times10^3$: a) $t/t_{ref} = 1.40$; b) $t/t_{ref} = 1.79$; c) $t/t_{ref} = 2.57$; d) $t/t_{ref} = 2.57$.

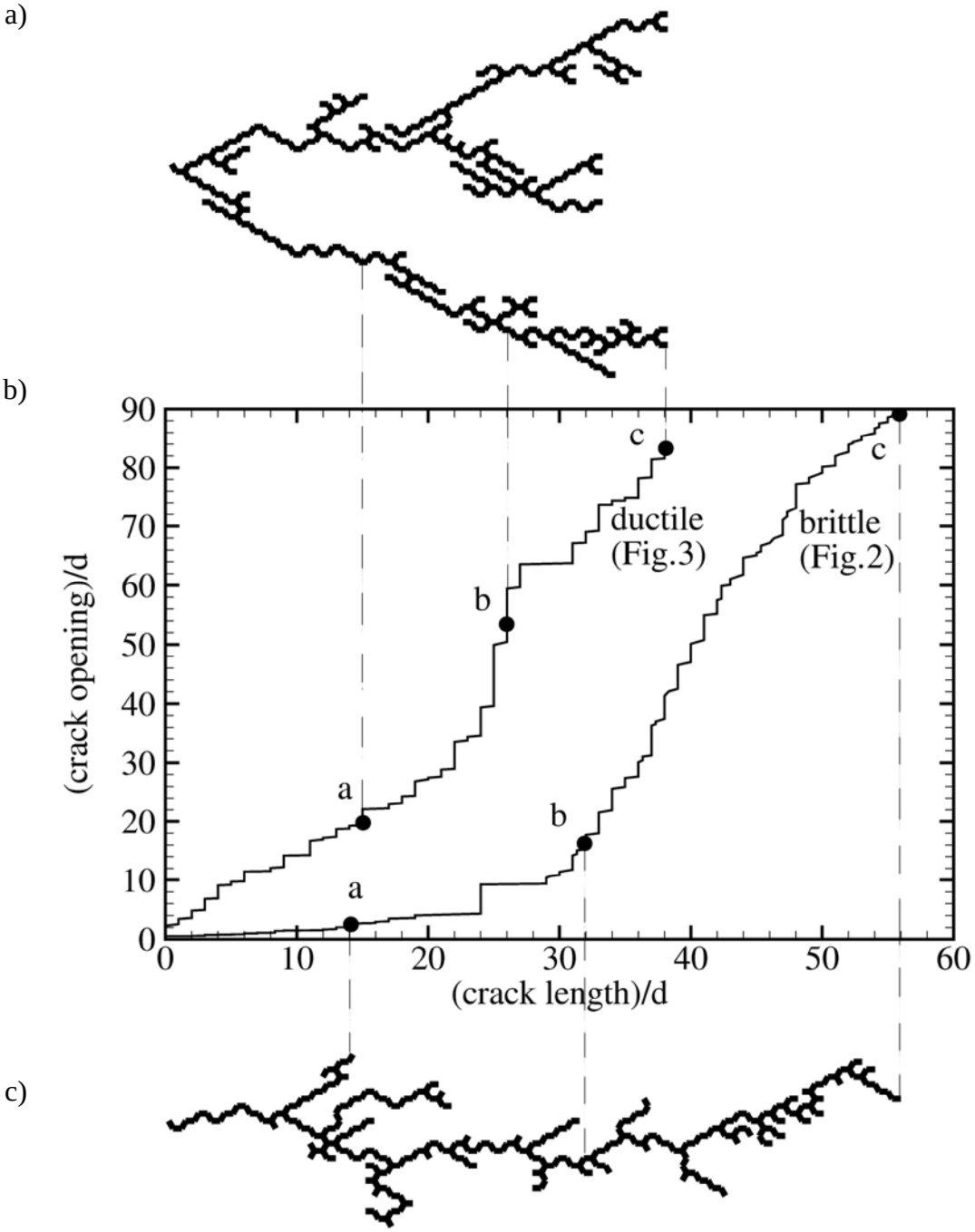

FIGURE 4. a) Crack topology for ductile fracture with $L/d = 0.042$, $F_n d^2 = 0.21\times10^3$; b) Correlation between brittle and ductile crack length against crack opening c) Crack topology for brittle fracture with $L/d = 0.19, F_n d^2 = 0.24\times10^4$.

a) $t/t_{ref} = 6.66\times10^{-2}$ b) $t/t_{ref} = 6.74\times10^{-2}$

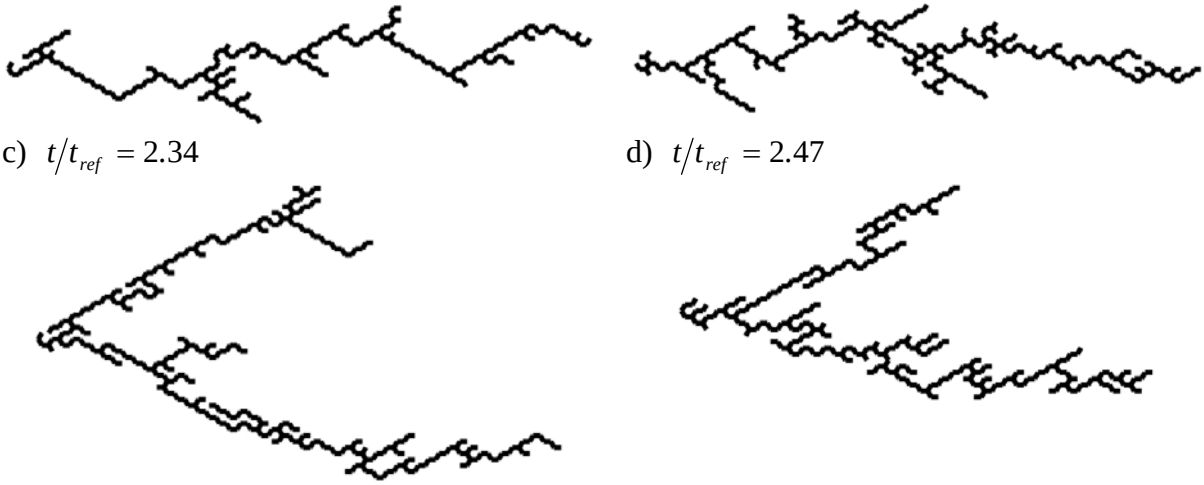

c) $t/t_{ref} = 2.34$ d) $t/t_{ref} = 2.47$

e)

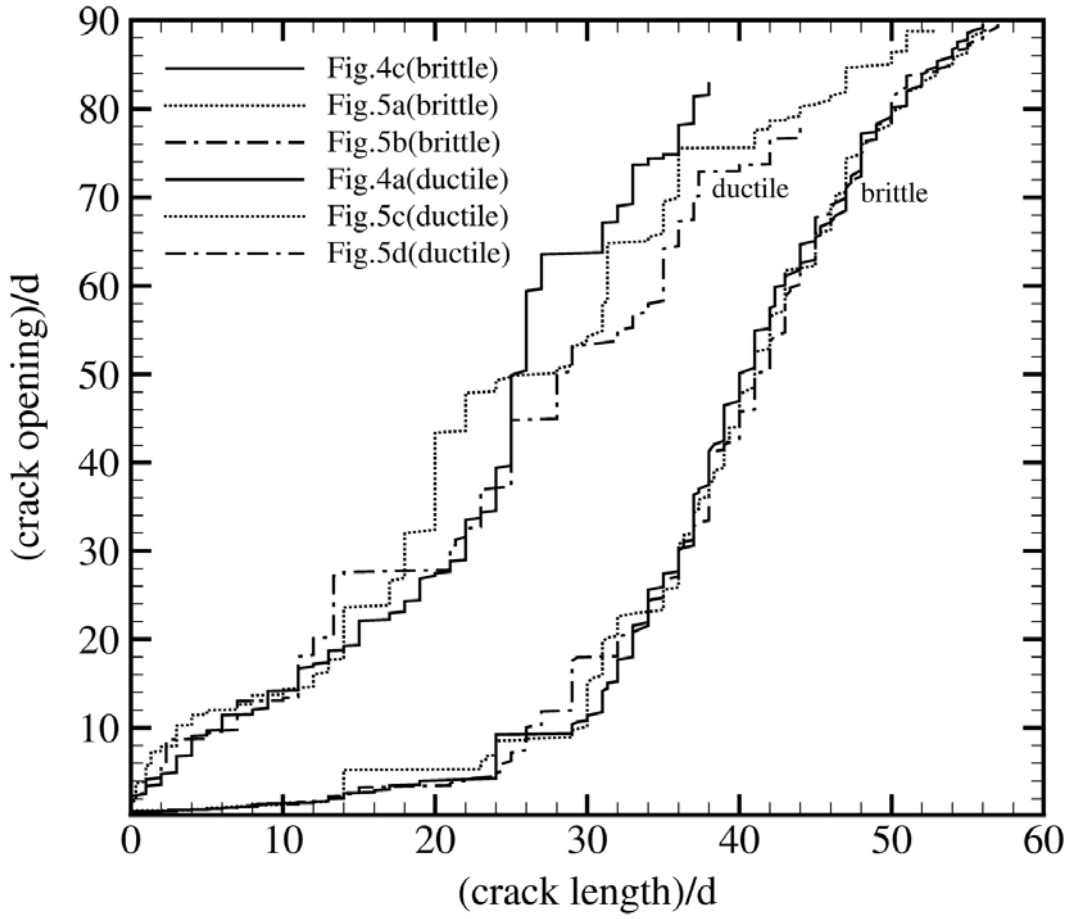

FIGURE 5. (a,b) Crack topology for brittle fracture with $L/d = 0.19$, $F_n d^2 = 0.24\times10^4$ with different random distributions of the creep parameter B and nucleated parameter F_n; (c,d) Crack topology for ductile fracture with $L/d = 0.042$, $F_n d^2 = 0.21\times10^3$ and different random distributions of creep parameter B and nucleated parameter F_n; e) Correlation between brittle and ductile crack length against crack opening for the different random distributions.

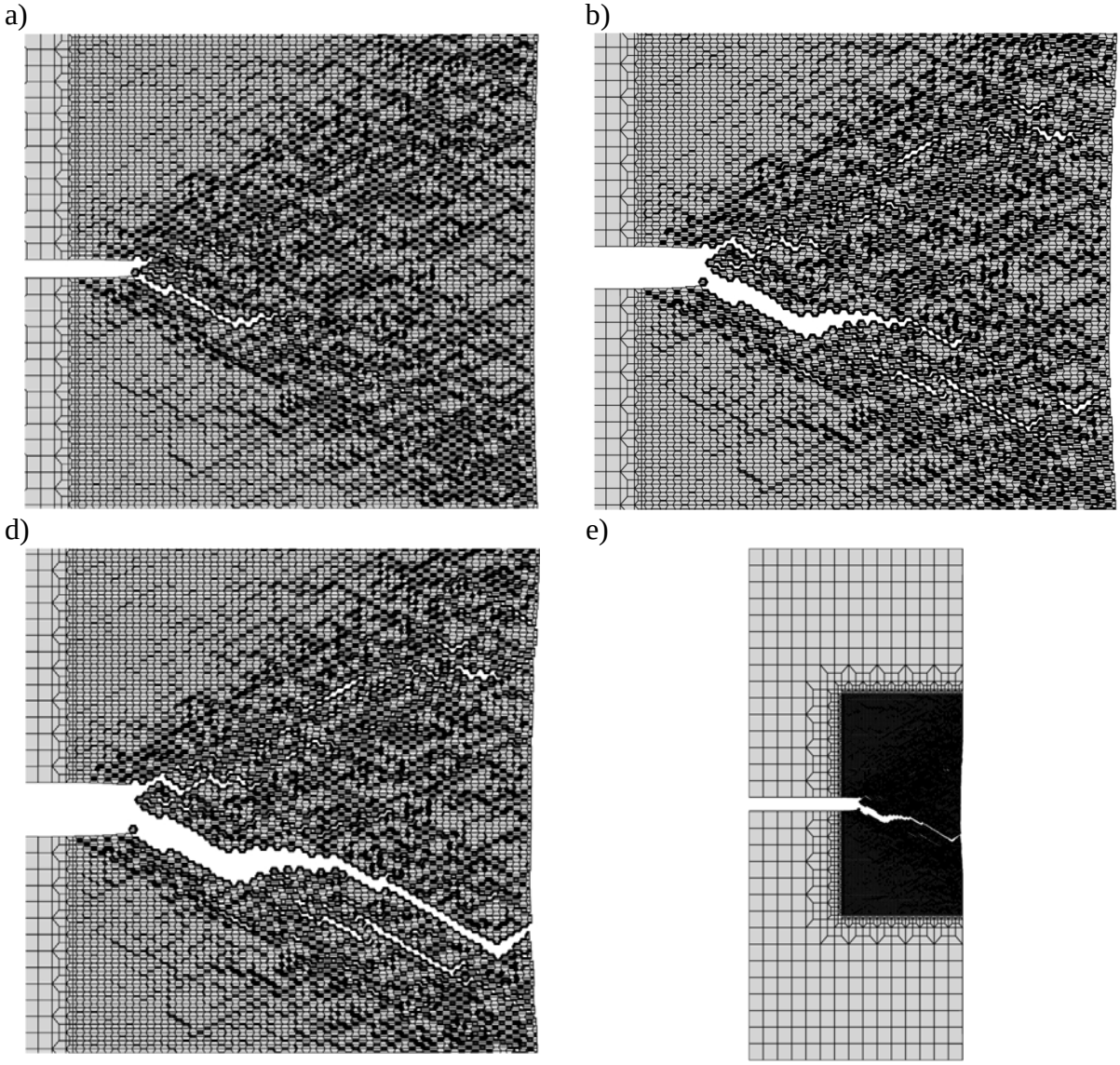

FIGURE 6. Snapshots during crack growth for displacement controlled boundary conditions with $L/d = 0.042,\ F_n d^2 = 0.21\times10^3$: a) $t/t_{ref} = 110.86$; b) $t/t_{ref} = 238.52$; c) $t/t_{ref} = 308.12$; d) $t/t_{ref} = 308.12$.

References

1. Mandelbrot B.B., *The Fractal Geometry of Nature,* Freeman, New-York, 1983
2. Bouchaud E., Lapasset G., Planes J., Naveos S., *Physical Review B,* vol. 48, 2917-2928, 1993
3. Onck P.R., Van der Giessen E., *J. Mech. Phys. Solids*, vol. 47, 99-139, 1999
4. Onck P.R., Nguyen B.N., Van der Giessen E., *J. Enging. Mat. and Techn.*, vol. 122 , 279-282, 2000